

# Optimization of Phase Shifted Long-Period Fiber Gratings for Multiband Rejection Filters

Isa Navruz and Ahmet Altuncu

**Abstract**—A new approach for designing multiband rejection filters is proposed based on the optimization of a periodically phase-shifted long period fiber grating (LPG). The validity of the method is demonstrated by performing simulations for the typical cases. It is shown that using the proposed synthesis method, spectral position, and bandwidth of the each reflection band can be controlled by varying the grating length and the phase shifting period. In addition, a desired number of rejection bands within the transmission spectrum can be generated using a phase-shifted LPG with an optimized phase shifting series. Furthermore, a number of unwanted rejection bands can easily be removed from the transmission spectrum by optimizing the phase shifting series.

**Index Terms**—Long period grating (LPG), multiband rejection filter, periodically phase-shifted grating, simulating annealing algorithm.

## I. INTRODUCTION

LONG period grating (LPG) which couple light from the fundamental mode into cladding modes propagating in the same direction has attracted great interest for fiber optical communications and sensor systems. They have been used as gain-flattening filters for erbium-doped fiber amplifiers [1]–[3], band rejection filters [4], dispersion compensators [5], add-drop multiplexers [6], [7], optical fiber polarizers [8] and also strain and temperature sensors [9]. Similar to fiber Bragg grating (FBG), one of the most significant properties of the LPGs is its tunability for the desired transmission characteristics by changing the grating parameters (refractive index modulation depth, grating phase, grating length, grating period, etc.).

In order to analyze an LPG, a coupled mode equation system must be solved using transfer matrix method. Using the appropriate grating parameters, the transmission characteristics of a uniform or a nonuniform LPG can easily be obtained. On the other hand, defining the required grating parameters leading to a desired transmission spectrum is not an analysis problem but it is a synthesis problem. In recent years, a lot of studies have been reported in literature on the synthesis of fiber Bragg gratings with long (LPG) or short period (FBG). The layer-peeling using inverse scattering method [10], the synthesis with Gel'fand Levitan–Marchenko coupled equations [11] and some optimization methods such as genetic algorithm [12], evolutionary programming [13], and simulated annealing [14] are the most popular

synthesis methods suggested and widely used in this subject. In the most of the studies reported on the synthesis of the LPGs, some applications such as single flat-band filter and optical amplifier gain flattening filter have been realized by tuning the coupling coefficient  $\kappa$  along the grating length which varies proportionally with the refractive index modulation depth. However, any synthesis study for the multiband rejection filters has not been reported in literature so far. A multiband rejection filter, in fact, composes of many rejection bands similar to the structure of an optical comb filter. The desired spectral response for such an optical filter can easily be obtained using the synthesis method of a periodically phase-shifted LPG (PPSLPG) proposed in this study. There are many analysis reported in literature on the phase-shifted LPGs [15]–[18] and its applications such as gain flattening fiber filters [19]–[21], different optical measurements [22]–[26] as bending curvature, temperature, transverse load, and refractive index. However, they are limited with constant phase applications and the spectra obtained have uniformly and evenly distributed rejection bands in an infinite bandwidth. In this paper, a new approach is proposed based on the optimization of the grating period by the synthesis of a periodically phase-shifted LPG including variable phase shifts. The validity of the method is demonstrated by performing simulations using the typical cases to compare the design with the target spectrum.

## II. THEORY

In a single-mode fiber LPG with a grating period of  $\Lambda$ , phase-matching condition between the guided fundamental mode and the forward propagating cladding modes is given by

$$\lambda_m = (n_{co} - n_{cl}^m)\Lambda \quad (1)$$

where  $n_{co}$  and  $n_{cl}^m$  are the effective refractive indexes of the fundamental and  $m$ th-order cladding modes, respectively, and  $\lambda_m$  is the resonance coupling wavelength. The refractive index variation in an LPG can be described as

$$n(z) = n_{co}(z) + \Delta n_{co} \cos\left(\frac{2\pi z}{\Lambda} + \phi(z)\right). \quad (2)$$

Here,  $\Delta n_{co}$  is the modulation depth of the refractive index and  $\phi(z)$  is the grating phase. A uniform LPG has a single resonant peak in the optical spectrum. The phase shifts added to a uniform grating affect its transmission spectrum. In Fig. 1, a schematic diagram of a periodically phase-shifted LPG which has  $N$  phase shifts in each phase shifting period is illustrated.

A phase shift through the LPG can be provided by inserting a length of unperturbed region. For example, a phase shift of  $2\pi$  or  $\pi$  can be obtained by adding a length of  $\Lambda$  or  $\Lambda/2$  into the LPG,

Manuscript received October 11, 2007; revised March 3, 2008. Published August 29, 2008 (projected).

I. Navruz is with the Department of Electronics Engineering, Ankara University, Ankara 06100, Turkey (e-mail: inavruz@eng.ankara.edu.tr).

A. Altuncu is with the Faculty of Engineering, Department of Electrical and Electronics, Dumlupınar University, Kütahya 43100, Turkey (e-mail: altuncu@du.edu.tr).

Digital Object Identifier 10.1109/JLT.2008.922297

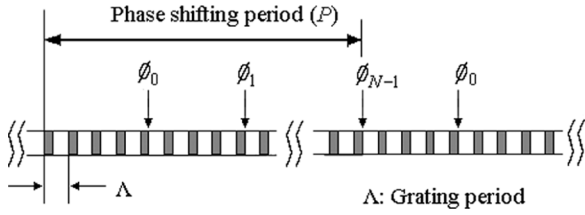


Fig. 1. Illustration of phase-shifted LPG.

respectively [19]. Alternatively, a phase shift can be provided using partial-etching technique which is a simple method [27]. Consequently, the fabrication process of the phase-shifted LPG is simpler than complex-structured fiber gratings.

The refractive index variation described in (2) can be rearranged for a periodically phase-shifted LPG as

$$n(z) = n_{co}(z) + \Delta n_{co} \operatorname{Re} \left\{ \exp \left[ i \left( \frac{2\pi z}{\Lambda} + \phi(z) \right) \right] \right\}. \quad (3)$$

Using the Fourier analysis, the effective index variation can be expressed by

$$n(z) = n_{co}(z) + \Delta n_{co} \operatorname{Re} \left\{ \sum_m F_m \exp \left[ i \left( \frac{2\pi z}{\Lambda} + \frac{2\pi m}{\Lambda_s} \right) \right] \right\}. \quad (4)$$

Here,  $\Lambda_s$  is the period of the grating phase shift  $\phi(z)$  and  $F_m$  is the complex discrete Fourier coefficients of  $\exp[i2\pi\phi(z)]$  and can be calculated using

$$F_m = \frac{1}{M} \sum_{k=0}^{N-1} \left[ \exp(i2\pi\phi(k)) \exp \left( -\frac{ik2\pi m}{M} \right) \right] \quad m = 0, 1, 2 \dots M-1. \quad (5)$$

In this paper, the number of Fourier coefficients  $M$  is assumed to be equal to the number of segments  $N$ . Note that (4) does not include the term  $\phi(z)$ . Instead, the complex Fourier coefficients  $F_m$  include  $\phi(z)$  and therefore represent the refractive index variation. The coupling coefficient is defined by  $\kappa = \eta\pi\Delta n/\lambda$  where  $\eta$  is the overall integral factor between the modes and  $\kappa$  is proportional to the refractive index modulation amplitude for a uniform LPG without phase shift. Therefore, the coupling coefficients of a periodically phase-shifted LPG can be rearranged as a series given as follows:

$$|\kappa_m| = |F_m \kappa|. \quad (6)$$

Here,  $\kappa_m$  and  $\kappa$  are the coupling coefficients of the phase-shifted and uniform LPG, respectively. All of the parameters except the grating phase are the same in both types.

Using coupling coefficient  $\kappa_m$ , the maximum transmissivity of the cladding mode (cross transmission) of the  $m$ th band in the transmission spectrum for the phase-shifted LPG can be expressed as [28]

$$t_{x,\max} = \sin^2 |\kappa_m L|. \quad (7)$$

Where  $L$  is the total grating length,  $t$  is the normalized cross transmission coefficient and subscript  $x$  denotes cross transmission in the cladding modes. At the wavelength in that the cross

transmission reaches to a maximum, the transmission of the fundamental mode becomes minimum. Using this data, the synthesis of the phase-shifted LPG can be realized by optimizing the phase of the grating.

For this purpose, first, a minimization problem that is going to get closer to a predefined target transmission spectrum for a periodically phase-sampled LPG has to be set up. The minimization problem can easily be set up using (7) as

$$C = \frac{1}{M} \sum_m W_m |t_x^{t \arg et} - t_x(\kappa_m)|. \quad (8)$$

Here,  $C$  is the cost function in minimization problem and  $W_m$  is the weight factor of cross transmission for  $m$ th band and can be selected as a positive number between 0 and 1. In order to solve this optimization problem, a simulating annealing algorithm [29] can be used. The simulating annealing algorithm is one of the fast and most robust optimization methods searching for global minima or maxima. The flowchart of the algorithm is illustrated in Fig. 2.

At the beginning of the algorithm, a target transmission that satisfies the desired spectral response should be defined. Since the maxima of an LPG's cross transmission wavelength spectrum can easily be calculated using (7), the cross mode transmission has been selected as a target instead of the fundamental mode transmission. When the target spectrum is going to be defined, the desired number of rejection bands in the wavelength spectrum and the cross transmission coefficients that are obtainable in practice for the related bands are considered.  $\phi^k$  is the phase shifting array with  $N$  components generated randomly at iteration  $k$ , and this algorithm tries to find out the optimum phase shifting array which gets it closer to the target at each iteration.  $T$  is the temperature control parameter and except the Markov chain iterations, it reduces slowly by the increasing iteration number. In any iteration not getting the closer to the target, the algorithm is rejected to converge to the local minima and supported to continue searching for a global minimum according to a probability defined by  $\exp(-\Delta C/T) > z$ . Here,  $\Delta C$  is the difference between the present cost and optimal cost. The iteration number at that the temperature control parameter remains constant is determined for the Markov chain transition probabilities. In the each iteration of the algorithm, the cross transmission spectrum of the phase-shifted LPG is calculated for the values only leading to a maximum. In other words, in contrast to the traditional grating synthesis methods, the whole wavelength spectrum is not calculated. Because, it is sufficient to make the maxima of the cross transmission spectrum correspond one by one to the channels at target spectrum. Therefore, this method is significantly fast and effective. The operation time of a phase-shifted LPG synthesis using simulation annealing algorithm takes 1–2 s using a standard PC.

### III. SIMULATION RESULTS

In this section, the simulation results are presented realized for a phase-shifted LPG whose grating phase is optimized by the optimization algorithm explained in the previous section. The parameters of the grating used in the simulations are an effective core mode index of 1.445, a cladding mode index of 1.4367, and a resonance wavelength of 1.55  $\mu\text{m}$ . Transmission

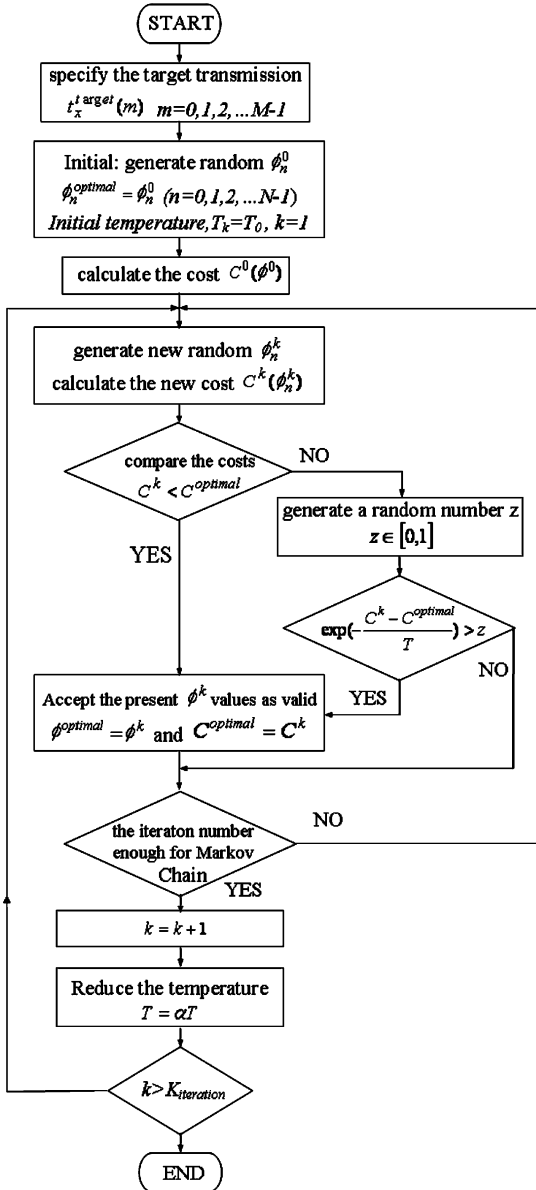


Fig. 2. Flowchart of the simulated annealing algorithm.

spectrum of the fundamental mode in an ordinary LPG having no phase-shift has a minimum in only one resonant wavelength and zero transmission exactly appears for the coupling coefficient  $\kappa_0 = \pi/(2L)$ . However, the spectrum of an LPG having phase-shifts can have minima at many wavelengths. However, these minima may not reach to zero for the coupling coefficient  $\kappa = \kappa_0$ . In the numerical simulations of a periodically phase-shifted LPG, first, a synthesis were realized using a phase shifting array with a phase shift number of  $N = 10$ . This array is separately optimized for each simulation regarding the desired spectral properties such as the quantity, the depth and the spectral positions of the rejection bands.

Fig. 3(a) illustrates the set of phase shifts per unit length of phase-shift period obtained by the numerical optimization of (8). The stairs in Fig. 3(a) represent the sudden phase shifts at the positions equally separated along the fiber grating length. In Fig. 3(b), the transmission spectrum of a phase-shifted LPG utilizing the calculated phase shifts is shown for a spectrum having

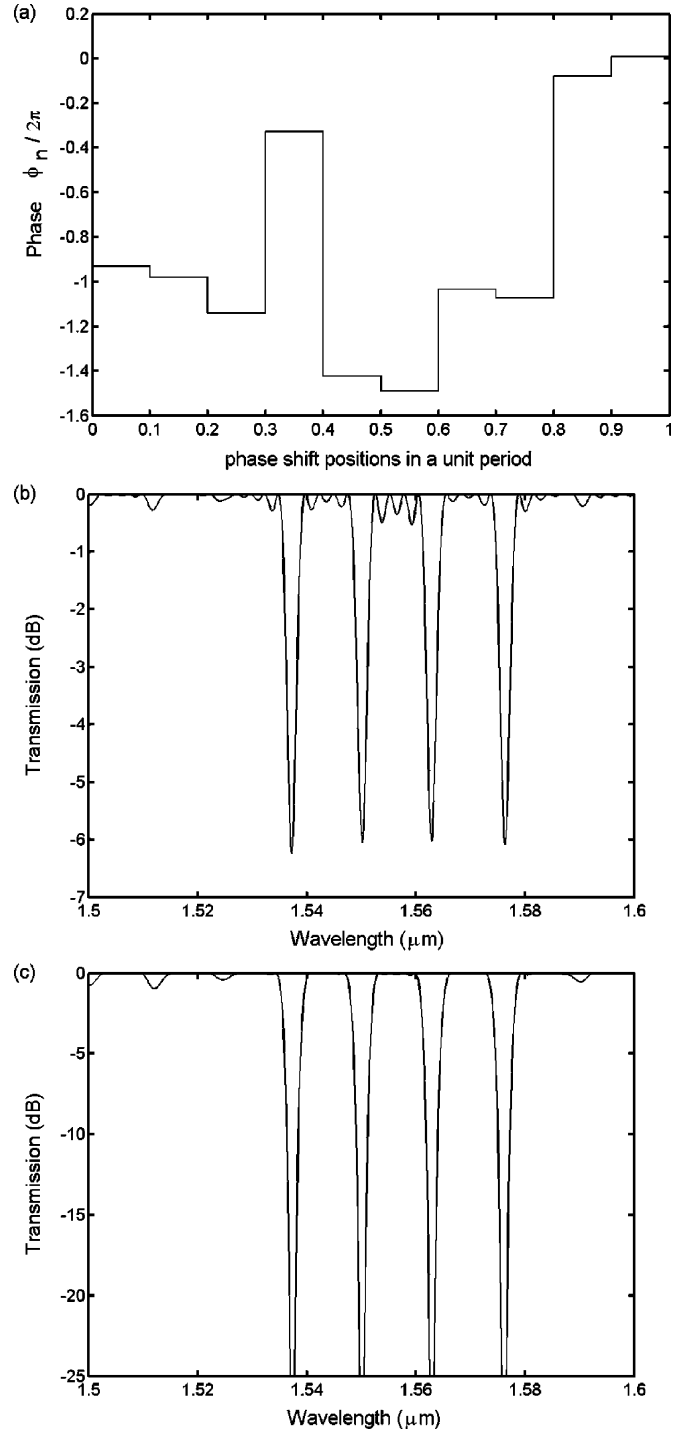


Fig. 3. Characteristics of a phase-shifted LPG synthesized specifically for four rejection bands. (a) The set of phase shifts per unit length of phase shift period. (b) The transmission spectrum without apodization ( $\kappa = \kappa_0$ ). (c) The transmission spectrum with Gaussian apodization ( $a = 6, \kappa = 3\kappa_0$ ). The other parameters:  $L = 12$  cm,  $P = 2.4$  cm,  $N = 10$ .

four rejection bands. In this synthesis, the length of the LPG is  $5 \cdot P$  and it includes  $5 \cdot N = 50$  phase shifts in total. Four rejection bands positioned with 12.5 nm separations are shown in the spectrum. In Fig. 3(b), the coupling coefficient is  $\kappa = \kappa_0$  and the rejection band depths are approximately  $-6$  dB. The number of ripples between two subsequent bands is 3 as clearly shown in Fig. 3(b). In order to reduce the amplitude of the ripples, the

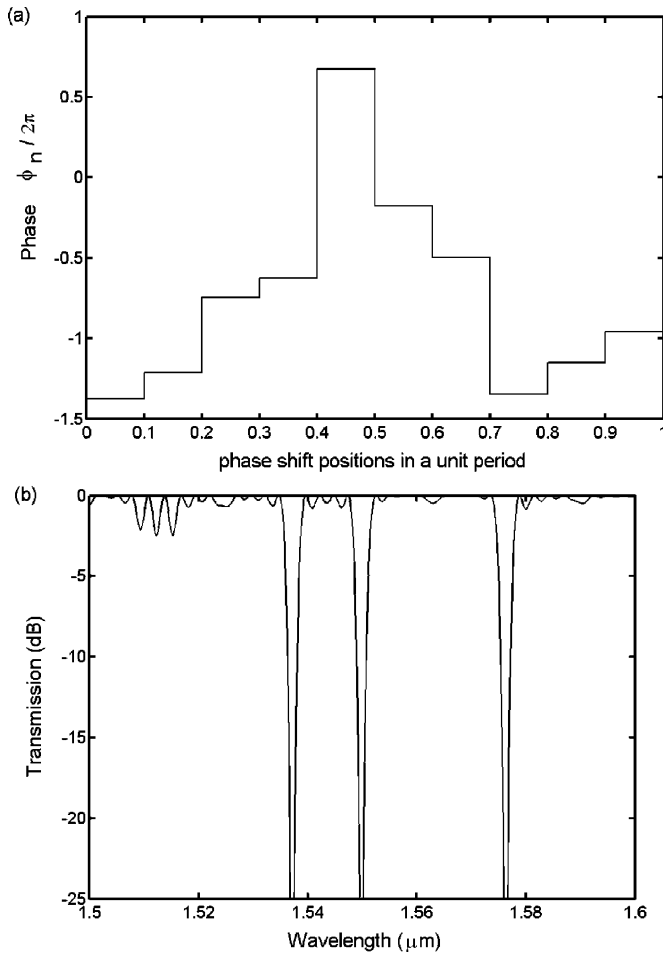


Fig. 4. Characteristics of a phase-shifted LPG synthesized without one of the rejection bands. (a) The set of phase shifts per unit length of phase shift period. (b) The transmission spectrum. Parameters:  $L = 12$  cm,  $P = 2.4$  cm,  $N = 10$ ,  $\kappa = 3.3\kappa_0$ ,  $a = 3$ .

refractive index of the grating can be apodized with a Gaussian index profile as

$$f(z) = \exp \left[ -a \left( \frac{z - \frac{L}{2}}{L} \right)^2 \right] \quad (9)$$

where  $a$  is the Gauss width parameter so that the width of the Gaussian index profile can be increased by increasing it. We have also observed that the Gaussian index apodization used to suppress the side lobes of the band in a single uniform grating also gives constructive results in the periodically phase shifted LPGs by suppressing the side lobes of the rejected channels. In Fig. 3(c), the reductions provided in the amplitude of the ripples as a result of the apodization are clearly shown. On the other hand, increasing the coupling coefficient to  $3\kappa_0$  has provided the depths of the rejection bands to be smaller than  $-25$  dB as shown in Fig. 3(c) which is the required value for practical applications.

It may also be desired for the grating given in Fig. 3 that the third rejection band overlaid in the  $1.55\text{-}\mu\text{m}$  window is removed. In this case, it is required to regenerate the shifting series. For this purpose, it is sufficient to re-optimize the phase-shifting series by determining an appropriate target spectrum fit to the desired spectrum. Fig. 4(a) and (b) illustrate the variation of the phase shift and the transmission spectrum of the

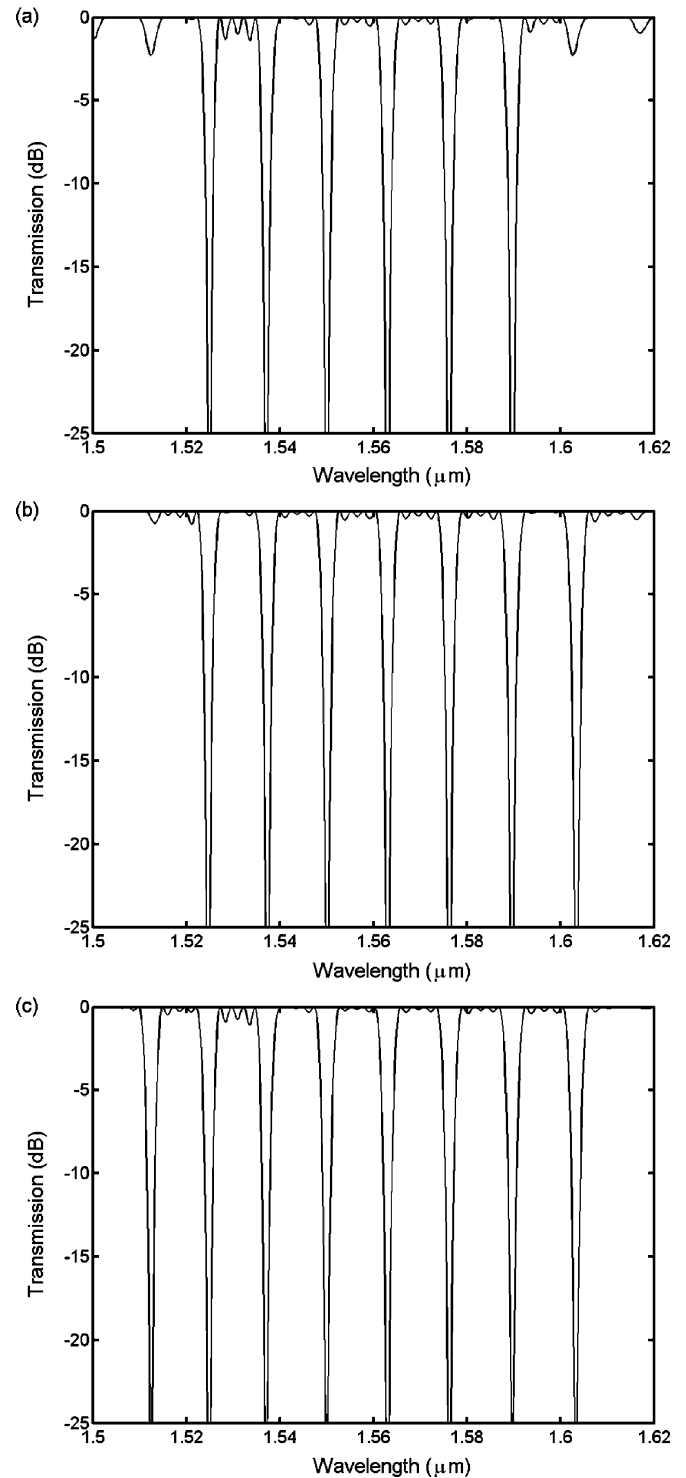


Fig. 5. Transmission spectra of the phase-shifted LPG with different number of rejection bands. (a) Six. (b) Seven. (c) Eight. Parameters:  $L = 12$  cm,  $P = 2.4$  cm,  $N = 10$ ,  $\kappa = 3.3\kappa_0$ ,  $a = 3$ .

grating obtained for the given synthesis example, respectively. It is clearly shown from the transmission spectrum of the grating that  $1562.5\text{-nm}$  rejection band has been removed although the other bands are not affected significantly.

In this simulation, it is assumed that  $M = N$  as it is used before. Therefore, if the phase shifting series consists of ten elements, the function of the target spectrum  $t_{x,\text{max}}$  will be an

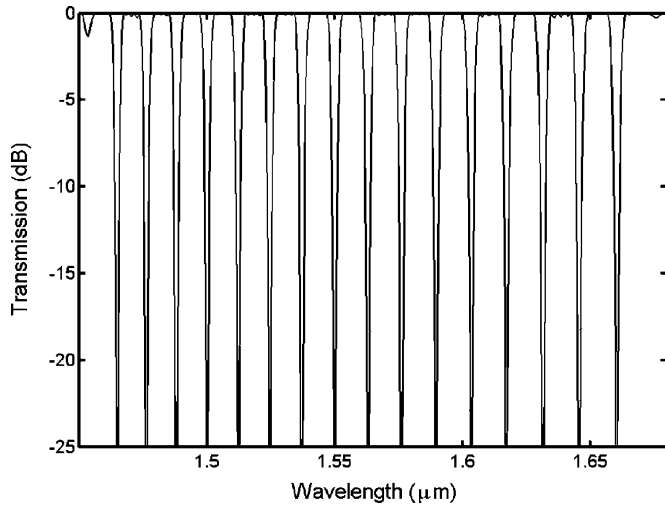


Fig. 6. Transmission spectrum of the phase-shifted LPG with 16 rejection bands. Parameters:  $L = 12$  cm,  $P = 2.4$  cm,  $N = 20$ ,  $\kappa = 6\kappa_0$ ,  $a = 6$ .

array with ten elements in which each of the elements corresponds to a maximum value in the cross mode transmission. It is thus understood that a maximum of ten rejection bands can be generated at the spectrum for  $N = 10$ . However, it is not usually desired to include the bands positioned at the right and left ends for spectral discrimination. In Fig. 5, the spectra of the phase-shifted LPG synthesis with six, seven, and eight rejection bands are shown.

In order to increase the number of channels at the spectra, phase shifting number  $N$  per period can be increased. For example, without changing the phase period  $P$ , it is possible to obtain up to 18 rejection bands at the transmission spectrum for the synthesis realized using  $N = 20$ . In Fig. 6, 16 similar rejection bands with equal spectral interval obtained by optimizing a phase-shifting series with 20 elements are shown.

In this study, finally, the effects of the phase-shifting period  $P$  and the grating length  $L$  on the transmission spectrum of a phase-shifted LPG are investigated. It is understood that both parameters have direct effects on the spectrum. The synthesis illustrated in Fig. 6 for  $P = 2.4$  cm was re-performed without changing the total grating length and total phase-shift number for  $P' = P/2$  and  $P' = 2 \cdot P$ , separately. Thus, the spectra shown in Fig. 7(a) and (b) have been obtained. As shown, there exists a linear inverse relationship between  $P$  and band intervals since when  $P$  increases the rejection bands get closer to each other leading to spectral densification. Fig. 7(c) illustrates the variation of the rejection band interval as an inverse function of the phase-shifting period,  $P$ , for  $N = 10$  (dashed line) and  $N = 20$  (solid line). Since two curves have coincided, the small graph sketched in Fig. 7(c) is placed to detail the presentation. As seen from Fig. 7(c), the band interval of the rejection bands changes almost linear with the inverse ratio of the phase-shifting period ( $1/P$ ) for both  $N = 10$  and  $N = 20$ . In addition, the variation of the phase-shifting period does not effect the bandwidth and the bandwidth of all rejection bands remains almost constant while band interval changes.

Varying the grating length without changing the phase shifting period has a linear effect on the rejection bandwidth. The spectra shown in Fig. 8(a) and (b) were obtained for

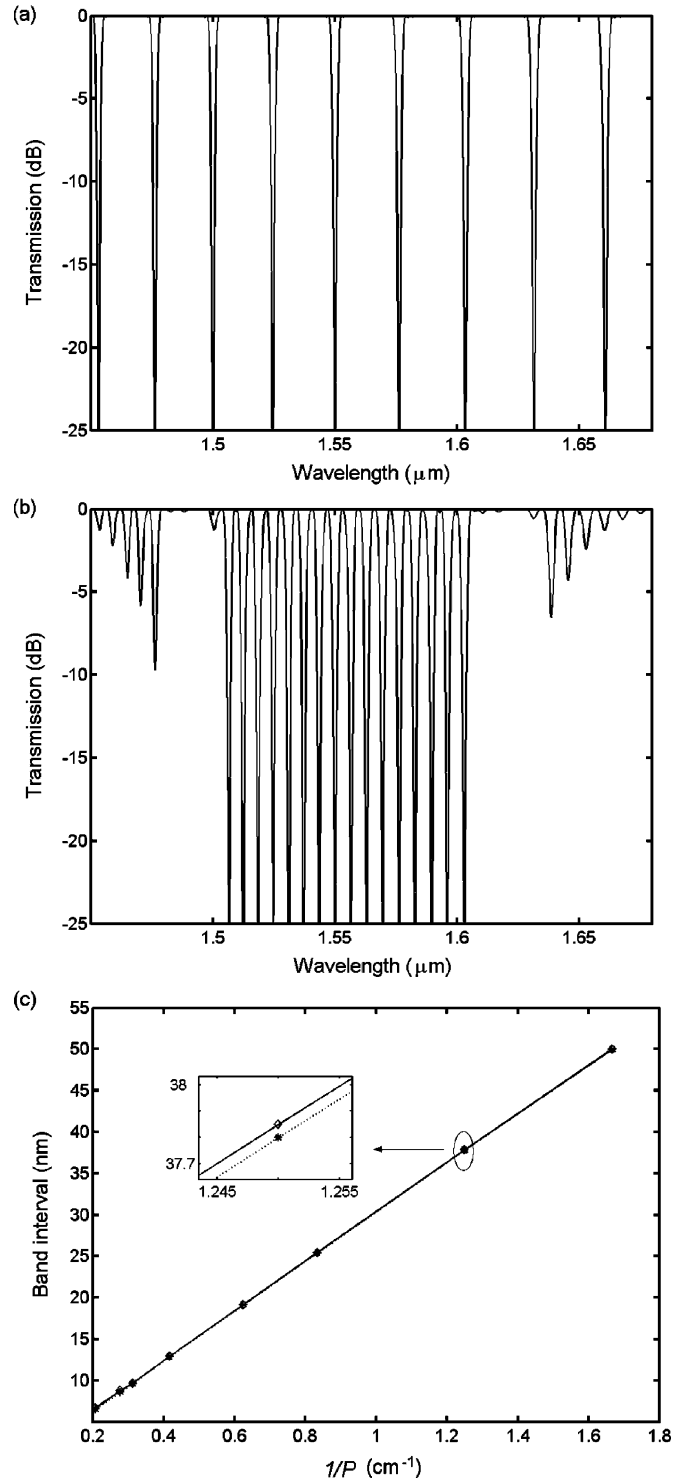


Fig. 7. (a) and (b) The phase-shifted LPG transmission spectra with 16 rejection bands in the case of  $N = 20$  for  $P = 1.2$  cm and  $P = 4.8$  cm, respectively, (c) band interval characteristics versus  $1/P$  for  $N = 10$  (dashed line) and  $N = 20$  (solid line). The other parameters:  $L = 14.4$  cm,  $\kappa = 3.3\kappa_0$ ,  $a = 3$  for  $N = 10$  and  $\kappa = 6\kappa_0$ ,  $a = 6$  for  $N = 20$ .

$L = 14.4$  cm and  $L = 7.2$  cm, respectively, and  $P$  was 2.4 in both spectra. As can be notified from the spectra, reducing grating length leads to an increase in bandwidth without affecting the spectral positions of the rejection bands or vice versa. Fig. 8(c) shows the variation of the channel bandwidth for the grating lengths changing from 7.2 to 19.2 cm and for

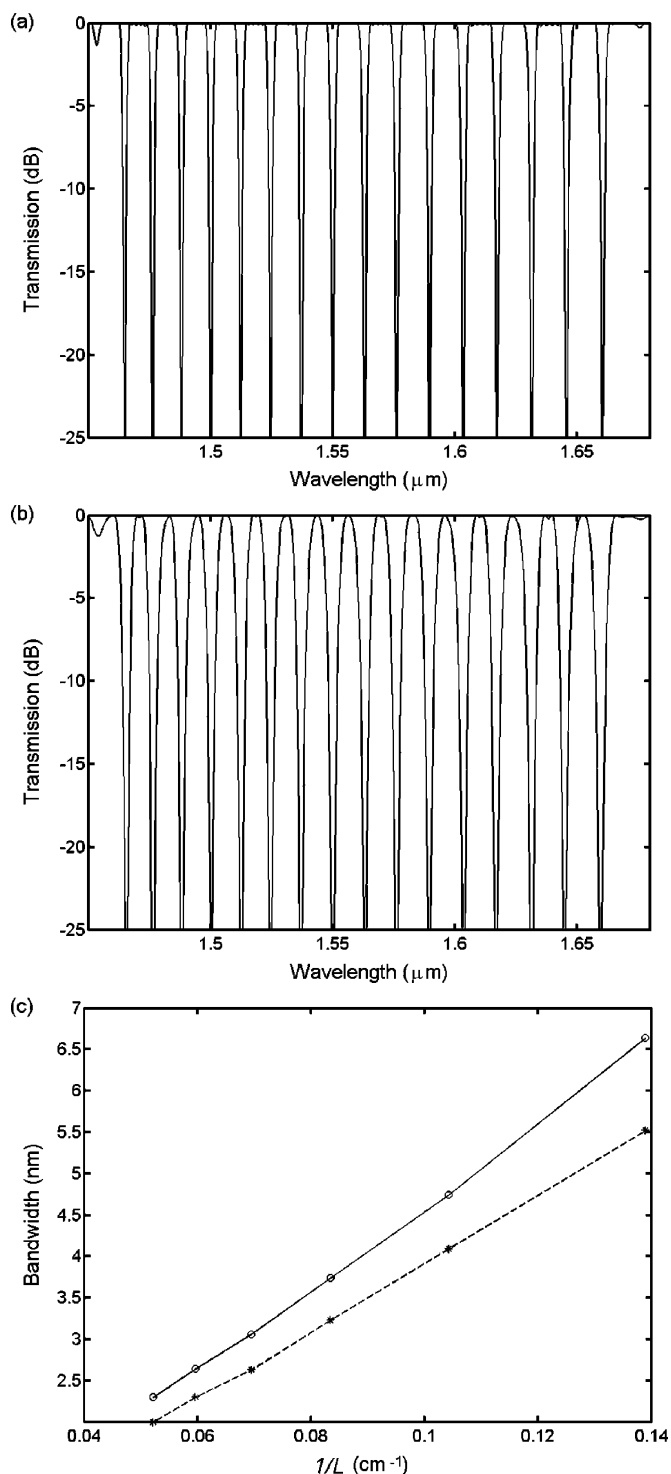


Fig. 8. (a) and (b) Phase-shifted LPG spectra with 16 rejection bands for different  $L$  values (a)  $L = 14.4$  cm, (b)  $L = 7.2$  cm, (c) bandwidth characteristics versus  $L$  for  $N = 10$  (dashed line) and  $N = 20$  (solid line). The other parameters:  $P = 2.4$  cm,  $\kappa = 3.3\kappa_0$ ,  $a = 3$  for  $N = 10$ ,  $\kappa = 6\kappa_0$ ,  $a = 6$  for  $N = 20$ .

a constant phase-shifting period. The dashed and solid curves in the figure represent the bandwidth characteristics for the phase-shifting numbers  $N = 10$  and  $N = 20$ , respectively. It is seen that the bandwidth characteristics changes nearly linearly with the inverse of the grating length ( $1/L$ ). It can also be concluded from this figure that the band interval and the band

position of each band in the spectrum almost remains constant while bandwidth changes. Consequently, the grating length and the phase-shifting period strongly affect the bandwidth and band interval of rejection bands in the spectrum, respectively, for both  $N = 10$  and  $N = 20$ .

#### IV. CONCLUSION

In conclusion, the spectral position and bandwidth of the reflection bands can be controlled by varying the grating length and phase shifting period. In addition, a desired number of rejection bands within the transmission spectrum can be generated with a phase-shifted LPG that uses optimized phase shifting series. By further optimization of the phase shifting series, the rejection band or bands that are not desired to be included within the spectrum can easily be removed.

#### REFERENCES

- [1] A. M. Vengsarkar *et al.*, "Long-period fiber-grating-based gain equalizers," *Opt. Lett.*, vol. 21, pp. 336–338, Mar. 1996.
- [2] M. K. Pandit, K. S. Chiang, Z. H. Chen, and S. P. Li, "Tunable long-period fiber gratings for EDFA gain and ASE equalization," *Microw. Opt. Technol. Lett.*, vol. 25, no. 3, pp. 181–184, May 2000.
- [3] R. Singh, Sunanda, and E. K. Sharma, "Gain flattening by long period gratings in erbium doped fibers," *Opt. Commun.*, vol. 240, pp. 123–132, Oct. 2004.
- [4] A. M. Vengsarkar, P. J. Lemaire, J. B. Judkins, V. Bhatia, T. Erdogan, and J. E. Sipe, "Long-period fiber gratings as band rejection filters," *J. Lightw. Technol.*, vol. 14, pp. 58–65, Jan. 1996.
- [5] M. Das and K. Thyagarajan, "Dispersion compensation in transmission using uniform long period fiber gratings," *Opt. Commun.*, vol. 190, pp. 159–163, Apr. 2001.
- [6] V. Grubsky, D. S. Starodubov, and J. Feinberg, "Wavelength-selective coupler and add-drop multiplexer using long-period fiber gratings," in *Tech. Dig. OFC2000*, 2000, pp. 28–30.
- [7] J. F. Huang, Y. J. He, and Y. L. Lo, "Bandwidth analysis of long-period fiber grating for high-order cladding mode and its application to optical add-drop multiplexer," *Opt. Eng.*, vol. 45, no. 12, Dec. 2006, 125001.
- [8] B. Ortega, L. Dong, W. F. Liu, J. P. de Sandro, L. Reekie, S. I. Tsypina, V. N. Bagratashvili, and R. I. Laming, "High-performance optical fiber polarizers based on long-period gratings in birefringent optical fibers," *IEEE Photon. Technol. Lett.*, vol. 9, no. 10, pp. 1370–1372, Oct. 1997.
- [9] V. Bhatia and A. M. Vengsarkar, "Optical fiber long-period grating sensors," *Opt. Lett.*, vol. 21, pp. 692–694, May 1996.
- [10] L. Wang and T. Erdogan, "Layer peeling algorithm for reconstruction of long-period fibre gratings," *Electron. Lett.*, vol. 37, no. 3, pp. 154–156, Feb. 2001.
- [11] E. Peral, J. Capmany, and J. Marti, "Iterative solution to the Gel'Fand–Levitan–Marchenko coupled equations and application to synthesis of fiber gratings," *IEEE J. Quantum Electron.*, vol. 32, pp. 2078–2084, Dec. 1996.
- [12] J. Skaar and K. M. Risvik, "A genetic algorithm for the inverse problem in synthesis of fiber gratings," *J. Lightw. Technol.*, vol. 16, no. 10, pp. 1928–1932, Oct. 1998.
- [13] C. L. Lee and Y. Lai, "Long-period fiber grating filter synthesis using evolutionary programming," *Fiber and Integrated Opt.*, vol. 23, pp. 249–261, Jul. 2004.
- [14] I. Navruz and N. F. Guler, "Optimization of reflection spectra for phase-only sampled fiber Bragg gratings," *Opt. Commun.*, vol. 271, pp. 119–123, Mar. 2007.
- [15] H. Ke, K. S. Chiang, and J. H. Peng, "Analysis of phase-shifted long-period fiber gratings," *IEEE Photon. Technol. Lett.*, vol. 10, no. 11, pp. 1596–1598, Nov. 1998.
- [16] Y. Liu, J. A. R. Williams, L. Zhang, and I. Bennion, "Phase shifted and cascaded long-period fiber gratings," *Opt. Commun.*, vol. 164, pp. 27–31, Jun. 1999.
- [17] L. R. Chen, "Phase-shifted long-period gratings by refractive index-shifting," *Opt. Commun.*, vol. 200, pp. 187–191, Dec. 2001.
- [18] F. Y. Chan and K. S. Chiang, "Analysis of apodized phase-shifted long-period fiber gratings," *Opt. Commun.*, vol. 244, pp. 233–243, Jan. 2005.
- [19] Y. Zhu, P. Shum, C. Lu, B. M. Lacquet, P. L. Swart, and S. J. Spammer, "EDFA gain flattening using phase-shifted long-period grating," *Microw. Opt. Technol. Lett.*, vol. 37, no. 2, pp. 153–157, Apr. 2003.

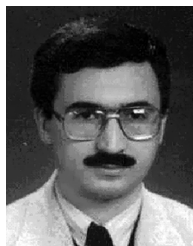
- [20] Y. Zhu *et al.*, "Device for concatenation of phase-shifted long-period grating and its application as gain-flattening fiber filter," *Opt. Eng.*, vol. 42, no. 5, pp. 1445–1450, May 2003.
- [21] J. R. Qian and H. F. Chen, "Gain flattening fibre filters using phase-shifted long period fibre gratings," *Electron. Lett.*, vol. 34, no. 11, pp. 1132–1133, May 1998.
- [22] Y. G. Han *et al.*, "Fibre-optic sensing applications of a pair of long-period fibre gratings," *Meas. Sci. Technol.*, vol. 12, pp. 778–781, Jul. 2001.
- [23] O. Frazão *et al.*, "All-fiber Mach-Zehnder curvature sensor based on multimode interference combined with a long period grating," *Opt. Lett.*, vol. 32, no. 23, pp. 3074–3076, Nov. 2007.
- [24] R. Falate *et al.*, "Bending sensitivity dependent on the phase-shift imprinted in the long-period fibre gratings," *Meas. Sci. Technol.*, vol. 18, no. 10, pp. 3123–3130, Sep. 2007.
- [25] Y. G. Han, J. H. Lee, and S. B. Lee, "Discrimination of bending and temperature sensitivities with phase-shifted long-period fiber gratings depending on initial coupling strength," *Opt. Express*, vol. 12, no. 14, pp. 3204–3208, Jul. 2004.
- [26] R. Falate *et al.*, "Refractometric sensor based on a phase-shifted long-period fiber grating," *Appl. Opt.*, vol. 45, no. 21, pp. 5066–5072, Jul. 2006.
- [27] K. W. Chung and S. Yin, "Design of a phase-shifted long-period grating using the partial-etching technique," *Microw. Opt. Technol. Lett.*, vol. 45, no. 1, pp. 18–21, Apr. 2005.
- [28] T. Erdogan, "Fiber grating spectra," *J. Lightw. Technol.*, vol. 15, no. 8, pp. 1277–1294, Aug. 1997.
- [29] S. Kirkpatrick, C. D. Gelatt, and M. P. Vecchi, "Optimization by simulated annealing," *Science*, vol. 220, pp. 671–680, May 1983.



fiber gratings.

**Isa Navruz** was born in Çankırı, Turkey, in 1974. He received the B.Sc. degree in electrical and electronics engineering from Dokuz Eylül University, Izmir, Turkey, in 1995 and the M.Sc. and Ph.D. degrees from Gazi University, Ankara, Turkey, in 2000 and 2006, respectively.

He is currently a Lecturer with the Department of Electronics Engineering, Ankara University. His research interests include the design and characterization of fiber gratings, optical filters, modeling, and simulation of light propagation in optical fiber and



**Ahmet Altuncu** was born in Afyonkarahisar, Turkey, in 1967. He received the B.Sc. degree in electronics engineering from Uludag University, Bursa, Turkey, in 1988 and the Ph.D. degree in electronics systems engineering from University of Essex, Essex, U.K., in 1998.

He is currently an Associate Professor and the head of Photonics Systems Research Group in Dumlupınar University, Kütahya, Turkey. His research interests include the design and characterization of wideband erbium-doped fiber amplifiers,

ASE sources and tunable fiber lasers, modeling and simulation of linear and nonlinear pulse propagation in optical fiber, and optical fiber sensors. He has authored and coauthored over 30 technical papers.